# ANTIMICROBIAL EFFICACY OF TILIROSIDE DERIVED FROM CORDIA MACLEODII AGAINST *KLEBSIELLA PNEUMONIAE*


**Abstract**

Antibiotic resistance is a global healthcare threat that has limited the effective life span of commercial medications. Medicinal plants are the reservoir of bioactive compounds that have antibacterial and antibiofilm activities and are potent source of new antimicrobial agents Therefore, the screening of plant derived phytochemicals has been increased significantly to access the hidden treasure to combat microbial infections. In the current study, preliminary analysis of the methanolic leaf extract of *Cordia macleodii* revealed the existence of various flavonoids including tiliroside. *In vitro* antimicrobial assay of methanolic extract and bioactive compound (Tiliroside) showed antibacterial and antibiofilm activity against MDR pathogen *Klebsiella pneumoniae* and its reference strain (MTCC 109). Methanolic leaf extract and tiliroside showed an 18 mm and 16 mm zone of inhibition against *K. pneumoniae* respectively. The MIC value of methanolic leaf extract and tiliroside was found to be 5 percent and 50mM respectively. Methanolic leaf extract as well as tiliroside at sub-MIC value significantly mitigated the biofilm formation. *In silico* molecular docking analysis of tiliroside against the targeted protein was also determined to predict the possible binding site. Transcriptomic analysis determined the significance of tiliroside in the reduced expression of certain genes (bssS and metE), which are involved in biofilm formation in *Klebsiella pneumoniae.* Tiliroside has lowest docking score of -6.163 Kcal/mol and -10.458 Kcal/mol against bssS and metE. Overall, the methanolic leaf extract of *C. macleodii* with varying degree of antimicrobial potency might be used as potent alternative to conventional antibiotics to combat MDR mediated infections.



**Keywords:** *Antibiofilm, Cordia macleodii, K. pneumoniae, Molecular docking, Tiliroside.*




## 1. INTRODUCTION

Rapid increased in antibiotic resistance is one of the major health threats making the therapeutic strategies more difficult and complicated (1). It not only exerts a selective pressure on the healthcare but also limits the effective life span of commercial drugs. Medicinal plants are the natural laboratories producing structurally diverse and functionally distinct complex compounds with pharmacological activities and less toxicity (2). These bioactive compounds have antibacterial and antibiofilm activities and can serve as templates for new antimicrobial agents. Further, natural products have gained significant popularity in therapeutics due to their traditional uses in folkloric medicine (3). Therefore, the screening of the plant derived phytochemicals is rapidly increasing to access the hidden treasure, which could be potential alternatives to commercial antibiotics for therapeutic applications against microbial infections (4).

The genus *Cordia* belonging to *Boraginaceae* family with more than 300 species has been widely investigated for their ethnobotanical and pharmacological properties (5). *C. macleodii* is an endangered medicinal plant found in the Gandhamardhan hills of Odisha (6), which possess various biological activities including anti-inflammatory, wound healing, antimicrobial, antioxidant, hepatoprotective and antivenom activities (7,8). Further, the analysis of leaves of *C. macleodi* reported the presence of several phytochemicals including high content of flavonoids with antimicrobial properties (7). However, the phytochemicals constituents of methanolic leaf extract of *C. macleodi* have not been fully assessed. The study was designed for photochemical characterization

of methanolic leaf extract of *C. macleodii* for the isolation of bioactive compounds. *In vitro* antimicrobial activities against *Klebsiella pneumoniae* of the leaf extract and identified bioactive compound (tiliroside) was evaluated. Transcriptomic analysis of the pathogenic bacteria (*K. pneumoniae*) was performed to determine the genes responsible for pathogenesis and biofilm formation. In addition, *in silico* molecular docking of tiliroside to predict the possible binding target and its binding mechanism of *K. pneumoniae* was performed.

## 2. MATERIALS AND METHODS

### 2.1 Sampling and Extraction

Fresh leaf samples of *C. macleodii* were collected from the Gandhamardhan hill, Odisha, India (Location: 20°42' - 21°00' North latitude and 82°41' - 83°05' East longitude), washed properly, chopped, dried and grinded into fine powder. About 500 gm of powdered sample was soaked with methanol for 72 hrs. Extract was filtered, rota-evaporated, air dried and stored at 4°C.

### 2.2 FTIR analysis

Leaf extract was analysed by FTIR within the spectral range 4000-400 $cm^{-1}$ using Bruker (Alpha II). Resolution was set at 4 $cm^{-1}$ with KBr beam splitter using DTGS detector along with their measurement through HGTR assembly (9).

### 2.3 HRMS analysis

Phytochemical composition in methanolic leaf extract of *C. macleodii* was performed using Exactive$^{TM}$ Plus Orbitrap HRMS integrated with tandem ultimate 3000 high-performance LC (Thermo Scientific, USA). 0.5 ml extract was suspended in 1.5 ml of methanol:water (1:1), centrifuged at 10000 rpm for 10 min at 4°C and filtered by 0.22 µM syringe. Filtrate of 0.5 ml was aspirated into DP ID vial for mass spectrometry analysis using Hypersil BDS C18 (250x2.1 mm, 5 µm) column. Sample was injected at 3 µl/min with 30°C column temperature and 700 bar pressure. Electrospray ionization was used to ionise molecule at 3eV for 15 mins and the positive and negative polarity were detected within (50-750) m/z range. Mass peak intensities were examined against five standard compounds with mass range of (50-500) m/z for converting peak intensities to concentration. Using python program and PubChem library parse the mass peaks were annotated having error range of (± 0.01) m/z (10).

### 2.4 Microbes and culture media

The bacterial strain (*Klebsiella pneumoniae*) was clinically isolated and identified by 16S rRNA sequencing. The standard strain of *K. pneumoniae* (MTCC 109) was received from IMTECH, Chandigarh. All the microbes were maintain using MHB.

### 2.5 Antibacterial assay

Antibacterial assay of methanolic leaf extract and tiliroside against *K. pneumoniae* and MTCC 109 was evaluated by well diffusion assay, which was performed following CLSI guidelines (11) and the diameter of zone of inhibition was measured. Microdilution method was used to determine MIC (3). Samples were dissolved in DMSO, serially diluted in MHB, 10 µl culture was inoculated and incubated for 16 hrs at 37°C. Well having culture without sample was treated as negative control. About 5 µl of 0.125% TTC was added and kept for 15 mins at 37°C and absorbance at 600 nm was taken. MIC value was determined taking the minimum concentration of sample with no change in change, which was subsequently utilized to compute the sub-MIC value.

### 2.6 Antibiofilm assay

#### 2.6.1 Qualitative Method

CRA method was performed to evaluate antibiofilm activity (12). Bacterial culture treated with sub-MIC level was streaked on solidified CRA plates and subjected to incubation for 24-48 hrs at 37°C. Culture without treatment was regarded as control. Further, test tube method was also carried out (13). Bacterial isolates (untreated and treated) were inoculated with TSB and incubated for 24 hrs at 37°C, stained with crystal violet for 15 mins after rinsing with PBS and air dried.

#### 2.6.2 Quantitative method

Polystyrene based 24-Microtiter plate (MTP) was performed for quantitative biofilm activity. Bacteria culture (with or without sub-MIC level) was inoculated in MH broth and incubated for 24 hrs at 37°C. Biofilm matrix developed was stained with 0.1% crystal violet for 20 mins, biofilms lining wall was solubilized with 95% ethanol and optical density at 540 nm was recorded (14).

#### 2.6.3 Microscopic studies

Microbial culture (0.5 McFarland standard) was added to 24-MTP containing sterile coverslip immersed in Luria-Bertani medium with or without sample and subjected to incubation incubated for 16 hrs at 37°C. Planktonic debris was removed via PBS wash and biofilm matrix developed was stained for 10 mins with 0.4% crystal violet for light microscopic whereas dyed with 0.01% acridine orange for 10 mins in dark for fluorescence microscopic studies (13).

### 2.7 Transcriptome analysis

Whole transcriptome sequencing was performed between untreated and treated with tiliroside against *K. pneumoniae*. Total RNA was isolated by Trizol method (Invitrogen) and amplified for illumina paired end sequencing library for high throughput sequencing. Purified cDNA library was assessed by Agilent bioanalyzer and HiSeq paired-end flow cell and massively-parallel sequencing on Illumina HiSeq 2000 for cluster generation. Pre-processed sequence reads by Trimmomatic and Printseq were aligned using TopHat integrated with Bowtie software, analyzed by Cufflinks to report expression of transcripts in FPKM. Differential gene expression was determined between treated and untreated using Cuffdiff and Cuffcompare. Differential expression was conducted using DESeq and edger, genes with fold change greater than 2 were analyzed by Cytoscape plugins, DAVID, STRING DB and IPA to obtain canonical pathways, 16 GO ontologies, protein network, gene clustering and protein identification.

### 2.8 In silico prediction and molecular docking

#### 2.8.1 Protein preparation

Proteins (bssS and metE) responsible for biofilm production and resistance in *K. pneumoniae* were used as targeted protein. PDB structures of proteins were pre-processed and protein preparation wizard was used to add the missing hydrogen atoms. Amino acids with missing side chain were identified and repaired using Prime. Protein structure was energy minimized by Macromodel, OPLS-2005 force field and Polak-Ribiere conjugate gradient algorithm (0.01 kcal/mol energy gradient).

#### 2.8.2 Preparation of molecular structure

Chemical structure of tiliroside was drawn by ChemDraw, which was then loaded into Maestro (Schrödinger). Energy minimization was performed using Macromodel and OPLS 2005 force field with Polak-Ribiere conjugate gradient algorithm. DFT with Becke's three-parameter exchange potential and Lee-Yang-Parr correlation function (B3LYP) using Jaguar was used for geometric optimization (15). Ligprep (Schrödinger) was used to generate various conformations of Tiliroside.

#### 2.8.3 Molecular docking

Blind docking strategy was adopted to investigate molecular interactions of tiliroside with different proteins in absence of co-crystal structures. Protein binding sites was predicted by SiteMap (Schrodinger) and receptor grid boxes having dimension (12Å x 12Å x 12Å) were created for each projected site using Glide grid-receptor program (15). The various conformations of tiliroside so generated were docked onto each of the predicted binding site using Glide XP algorithm and Glide $XP_{Score}$ function was evaluated. Best conformation of tiliroside with minimal docking score was selected for further study.

## 3. RESULT AND DISCUSSION

### 3.1 FTIR analysis

FTIR analysis of methanolic leaf extract of *C. macleodii* confirmed the existence of different chemical moieties with IR fingerprints ranging from 3289 $cm^{-1}$ to 1048 $cm^{-1}$ (Table 1). FTIR spectrum depicting different functional groups of bioactive constituents (Figure 1).

**Table 1. Details of bioactive phytochemical constituents identified through FTIR analysis of methanolic leaf extract of Cordia macleodii.**

| Sl. | Peak wave number (cm-1) | Types of vibration | Functional group | Bond |
|---|---|---|---|---|
| 1. | 3289.11 | Stretching | Alcohol | O-H |
| 2. | 2921.42 | Stretching | Alkane | C-H |
| 3. | 2851.76 | Stretching | Alkane | C-H |
| 4. | 1735.31 | Stretching | Carbonyl | C=O |
| 5. | 1604.05 | Stretching | Aromatic | C=C |
| 6. | 1519.10 | Banding | Nitro | N=O |
| 7. | 1442.66 | Stretching | Nitro | N=O |
| 8. | 1376.69 | Stretching | Nitro | N=O |
| 9. | 1245.63 | Banding | Amine | C-N |
| 10. | 1048.92 | Stretching | Amine | C-N |

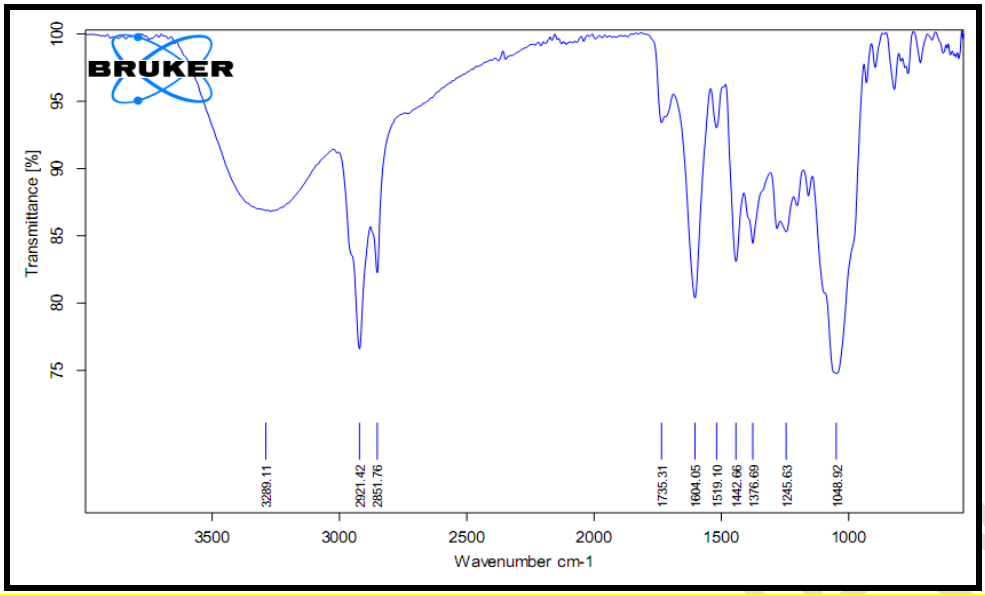


**Figure 1. FTIR spectrum of methanolic leaf extract of *Cordia macleodii* revealing the functional groups of phytochemical constituents.**

### 3.2 HRMS analysis

HRMS analysis revealed the occurrence of 19 compounds identified based on their chemical profiling based on fragmentation patterns, total ion chromatogram and comparison of spectra with NIST database and documented spectra (Supplementary Table 1). HRMS analysis reveals the prime bioactive compound (Tiliroside) with the highest peak area (13.6%) in methanolic extract of *C. macleodii* (Figure 2).

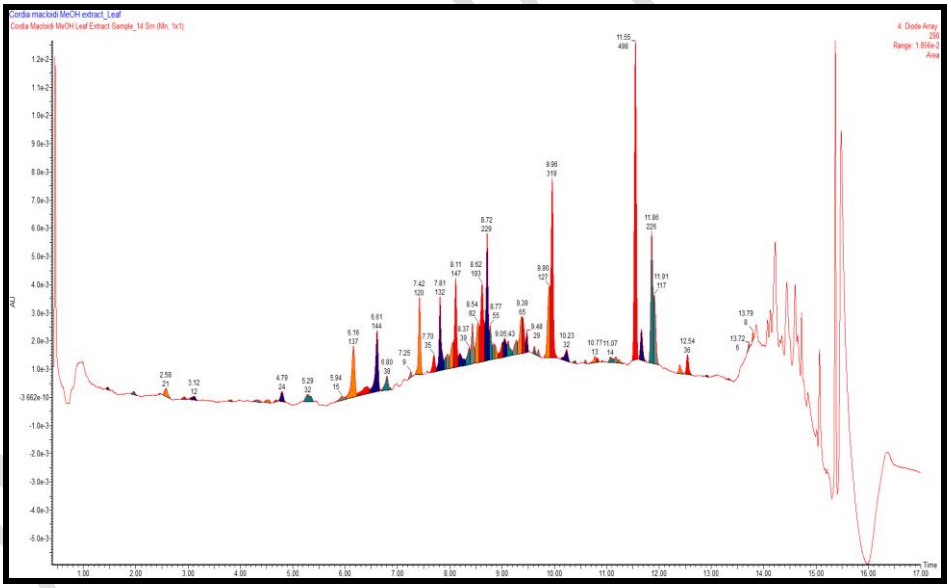

**Figure 2. Chromatogram of the crude methanolic leaf extract of Cordia macleodii indicating presence of several major phytochemicals.**

### 3.3 Antibacterial activity

MIC value of methanolic extract was found to be 5% whereas tiliroside was determined to be 50 mM against *K. pneumoniae* and MTCC 109 (Figure 3). Well diffusion assay revealed antibacterial property of methanolic leaf extract against *K. pneumoniae* and MTCC 109 with 18 mm and 24 mm zone of inhibition. Tiliroside showed reduced antibacterial activity compared to methanolic leaf extract in *K. pneumoniae* (16 mm) and MTCC 109 (20 mm).

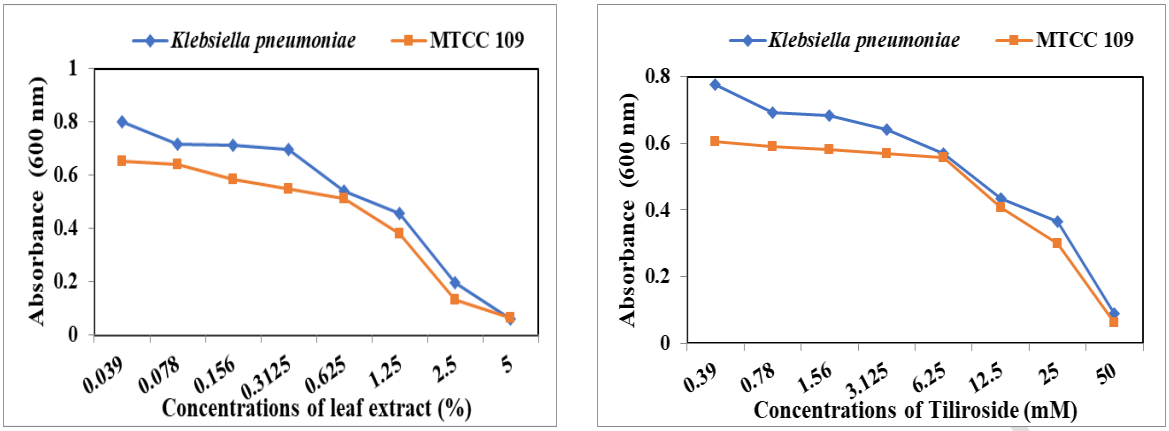


**Figure 3. MIC of (a) methanolic leaf extract of *Cordia macleodii* and (b) tiliroside against *K. pneumoniae* and reference strain (MTCC 109).**

## 3.4 Antibiofilm assay

### 3.4.1 Qualitative method

CRA method revealed the formation of crystalline black colonies in untreated control in *K. pneumoniae* and MTCC 109, which indicated profuse production of exopolysaccharide matrix for biofilm production (Figure 4). Significant decline in biofilm production was observed in treated strain of *K. pneumoniae* and MTCC 109 (supplemented with methanolic extract and tiliroside at sub-MIC value) indicating its antibiofilm activity (Figure 4a). Similar result was evident from test tube method (Figure 4b).

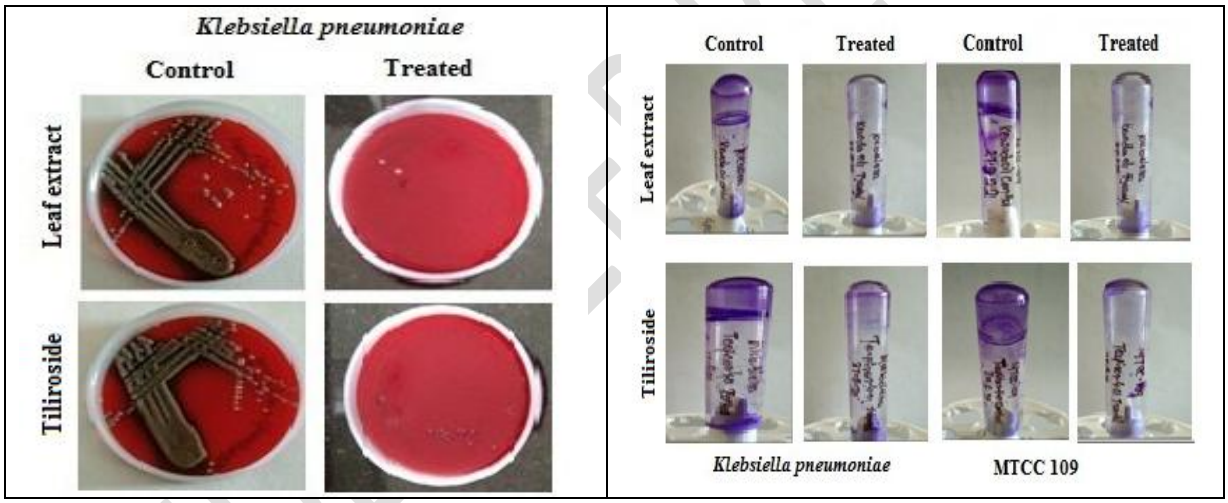


**Figure 4. Antibiofilm activity of methanolic leaf extract of *C. macleodii* and tiliroside at sub-MIC against *K. pneumoniae* and MTCC 109 based on (a) Congo red agar; (b) Test tube method.**

### 3.4.2 Quantitative assay

Relatively higher antibiofilm activity was observed by tiliroside compared to methanolic leaf extract of *C. macelodii* (Figure 5). Highest inhibitory effect towards biofilm formation was exhibited by tiliroside in *K. pneumoniae* (62.26 ± 5.29 %) and MTCC 109 (59.65 ± 4.68 %).

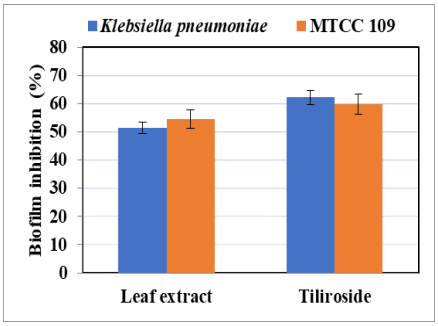


**Figure 5. Antibiofilm activity of methanolic leaf extract of *C. macleodii* and tiliroside at sub-MIC on biofilm formation in *Klebsiella pneumoniae* and MTCC 109.**

### 3.4.3 Microscopic studies

Light microscopic studies revealed significant decline in biofilm matrix in *K. pneumoniae* and MTCC 109 supplemented with sub-MIC of methanolic leaf extract and tiliroside compared to cells assemblage in untreated control (Figure 6a). Fluorescence microscopy revealed significant decline in aggregation of biofilm forming cells with disperse localization compared to thickened and aggregate biofilm in untreated control (Figure 6b).

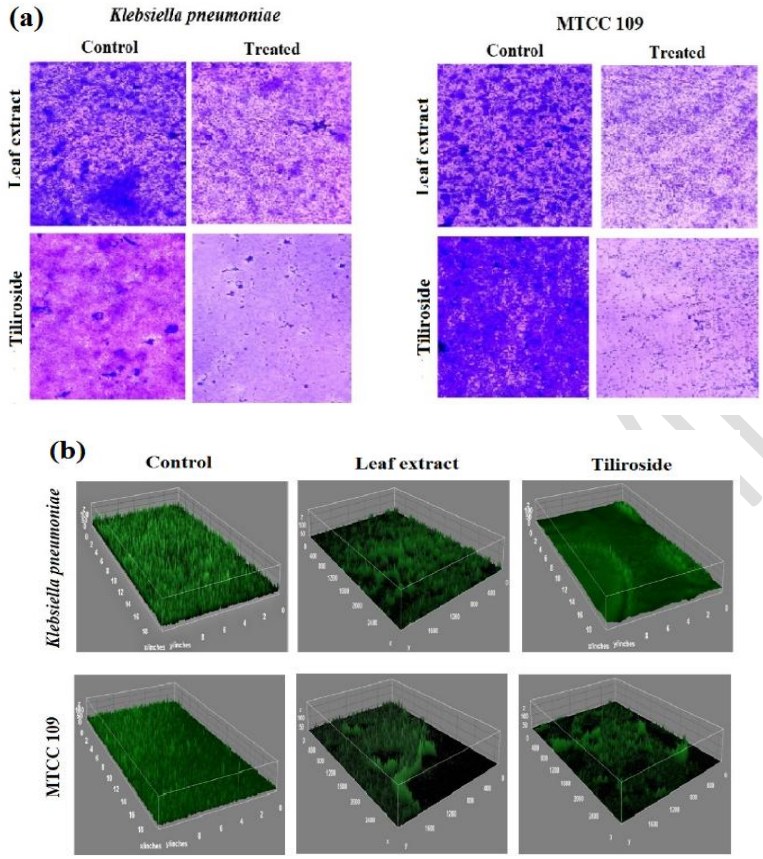


**Figure 6. Antibiofilm activities of methanolic leaf extract of *C. macleodii* and tiliroside at sub-MIC against *K. pneumoniae* and MTCC 109 based on (a) light microscopic and (b) fluorescence microscopic studies.**

## 3.5 Transcriptome analysis

### 3.5.1 Transcriptomic sequencing data analysis

Data of *K. pneumoniae* (Control_1 and Control_2) and *K. pneumoniae* treated with tiliroside (TIL_1 and TIL_2) were used for quality checking and trimming. Statistical percentage passed quality checking. Genome of *K. pneumoniae* was used as reference to align reads using HISAT2. The study indicated 99.98% and 100.00% reads obtained from Control_1 and Control_2 was mapped with reference genome, whereas 100% reads from TIL_1 and TIL_2 was mapped with reference genome. Mapping results with the statistical summary were presented (Table 2). Transcript abundances were calculated employing Cufflinks package. To identify various DEGs, FPKM were computed and Cuffdiff package was implemented. Considering the *q* value, the p value was modified. The number of DEGs found was depicted.

**Table 2. Statistical summary of the mapping results.**

| Alignment details | *Klebsiella pneumoniae* | | *Klebsiella pneumoniae /Tiliroside* | |
|---|---|---|---|---|
| | Control_1 | Control_2 | TIL_1 | TIL_2 |
| Total reads | 11380880 (100%) | 11380223 (100%) | 14104596 (100%) | 14942921 (100%) |
| Aligned 0 times | 11380800 (99.98%) | 11380223 (100%) | 14104596 (100%) | 14942921 (100%) |
| Aligned exactly 1 time | 88 (0%) | 72 (0%) | 232 (0%) | 224 (0%) |
| Aligned >1 times | 1751 (0.02%) | 35 (0%) | 469 (0%) | 70 (0%) |

### 3.5.2 PPI network analysis

PPI network analysis was performed using up-regulated genes (n = 4), which suggested the involvement of two genes (rpmC and SAXN108_2407) in signal pathways, that were merged using STRING to examine their relationship with DEGs. PPI network was also created using down-regulated genes (n = 11), integrated via STRING to explore interaction between DEGs involved in biofilm development.

### 3.5.3 Functional annotations of the up-regulated and down-regulated genes

The up-regulated genes in *K. pneumoniae* were identified after treated with methanolic leaf extract of *C. macleodii*. Functional annotations of genes (rpmC and SAXN108_2407) among four up-regulated genes were available. Besides, two genes (bssS and metE) among 11 down-regulated genes are directly associated with pathogenesis of *K. pneumoniae* through biofilm formation.

### 3.6 Molecular docking of tiliroside

Due to lack of its co-crystal structures, a blind docking strategy was followed to dock tiliroside to suitable binding site on the target proteins. Tiliroside has lowest docking score of -6.163 Kcal/mol and -10.458 Kcal/mol against bssS and metE (Table 3), which were well accommodated in binding cavity (Figure 6). Tiliroside involved hydrogen bonds with amino acids present at binding sites of bssS (Figure 7B) and metE protein (Figure 7D) along with several hydrophobic interactions (Figure 7).

**Table 3. Docking of tiliroside against binding sites onto proteins involved in biofilm production in pathogenic strain of *K. pneumoniae*.**

| Site ID | Site score | Volume $(Å)^3$ | Glide XP score (Kcal/mol) |
|---|---|---|---|
| **(a) bssS protein** | | | |
| 1 | 0.539 | 52.822 | -6.163 |
| **(b) metE protein (PDB ID: 3L7R)** | | | |
| 1 | 1.073 | 260 | -10.069 |
| 2 | 1.047 | 232 | -8.990 |
| 3 | 1.069 | 141 | -8.259 |
| 4 | 1.095 | 99 | -9.453 |
| 5 | 1.086 | 73 | -10.458 |

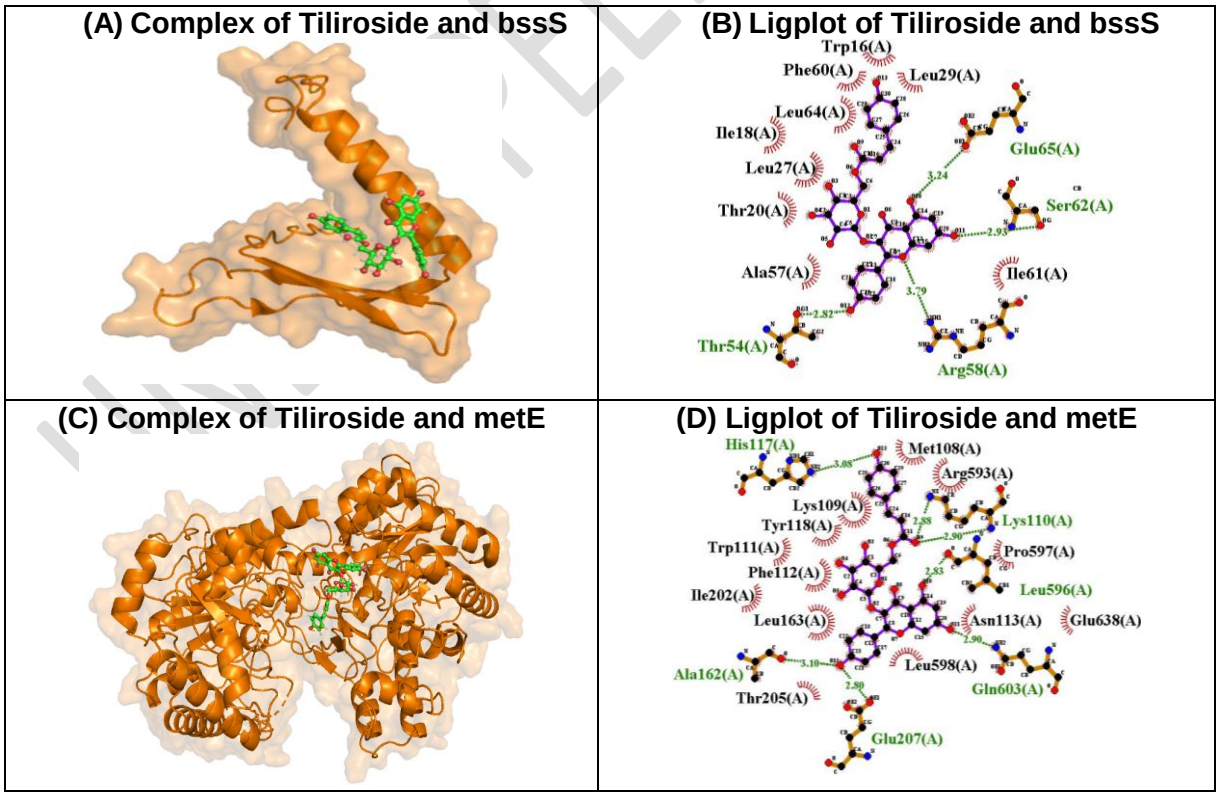


**Figure 7. Molecular docking of tiliroside onto proteins within the binding site of (A) bssS protein and (C) metE proteins. Ligplot illustrating interaction of tiliroside with amino acids at binding sites of (B) bssS; (D) metE proteins. Dotted (green) lines represent hydrogen bonds whereas curved (red) lines represent hydrophobic interactions.**

Efficacy evaluation of plant derived bioactive compounds is complicated and challenging due to chemical complexities, variability in structures and binding affinity with multiple target sites (16). Secondary metabolites derived from medicinal plant target microbes by the combined action of structurally distinct and functionally diverse compounds. Further, the target microbes are less likely to acquire resistance against combined action of plant derived bioactive compounds compared to single molecule. Hence, the plant bioactive compounds serve as a source for novel antimicrobial agents.

## 4. CONCLUSION

The aforementioned study revealed that the medicinal plant *C. macleodii,* possess good antimicrobial activity against the test bacterium. It also indicated that the biofilm inhibitory activity of methanolic leaf extract and isolated compound (tiliroside) that significantly reduce the formation of exopolysaccharides matrix in pathogenic microbes, highlighting their usefulness in healthcare sector. Further, *in silico* molecular docking of tiliroside reported highest binding affinity against metE protein (PDB ID: 3L7R) with docking score of -10.458 Kcal/mol, reflecting the potency of tiliroside in biofilm inhibition. Moreover, the study evident that tiliroside derived from the leaf extract of *C. macleodii* holds promise as a natural antimicrobial agent to combat microbial mediated disease, potentially reducing the reliance on commercial antibiotics and therby aiding in the mitigation issues such as antibiotic resistance.

## REFERENCES


1. Kalpana S, Lin WY, Wang YC, Fu Y, Lakshmi A, Wang HY. Antibiotic Resistance Diagnosis in ESKAPE Pathogens—A Review on Proteomic Perspective. Diagnostics. 2023; 13(6): 1014.
2. Anza M, Endale M, Cardona L, Cortes D, Eswaramoorthy R, Zueco J, Trelis M, Abarca B. Antimicrobial activity, in silico molecular docking, ADMET and DFT analysis of secondary metabolites from roots of three ethiopian medicinal plants. Adv Appl Bioinforma Chem. 2021; 117-132.
3. Sánchez E, Morales CR, Castillo S, Leos-Rivas C, García-Becerra L, Martínez DMO. Research Article Antibacterial and Antibiofilm Activity of Methanolic Plant Extracts against Nosocomial Microorganisms. 2016.
4. AlSheikh HMA, Sultan I, Kumar V, Rather IA, Al-Sheikh H, Tasleem Jan A, Haq QMR. Plant-based phytochemicals as possible alternative to antibiotics in combating bacterial drug resistance. Antibiotics. 2020; 9(8): 480.
5. Oza MJ, Kulkarni YA. Traditional uses, phytochemistry and pharmacology of the medicinal species of the genus Cordia (Boraginaceae). J Pharm Pharmacol. 2017; 69(7): 755-789.
6. Nariya PB, Shukla VJ, Acharya RN. Phytochemical screening and in vitro evaluation of free radical scavenging activity of Cordia macleodii bark. (HOOK. F. & THOMSON). Free Radicals and Antioxidants. 2012; 2(3): 36-40.
7. Qureshi NN, Kuchekar BS, Logade NA, Haleem MA. Antioxidant and hepatoprotective activity of Cordia macleodii leaves. Saudi Pharm J. 2009; 17(4): 299-302.
8. Bhide B, Acharya RN, Naria P, Pillai APG, Shukla VJ. Pharmacognostic evaluation of Cordia macleodii Hook. stem bark. Pharmacogn J 2011; 3(26): 49-53.
9. Sravan Kumar S, Manoj P, Giridhar P. Fourier transform infrared spectroscopy (FTIR) analysis, chlorophyll content and antioxidant properties of native and defatted foliage of green leafy vegetables. J Food Sci Technol. 2015; 52:8131-9.
10. Marulasiddaswamy KM, Nuthan BR, Sunilkumar CR, Bajpe SN, Kumara KK, Sekhar S, Kini KR. HR-LC-MS based profiling of phytochemicals from methanol extracts of leaves and bark of *Myristica dactyloides* Gaertn. from Western Ghats of Karnataka, India. J App Biol Biotechnol. 2021; 9(5):124-35.
11. CLSI. Performance Standards for Antimicrobial Disk Susceptibility Tests, 12th ed.; CLSI Document M02-A12; CLSI: Wayne, PA, USA (2015).
12. Chhibber S, Gondil VS, Sharma S, Kumar M, Wangoo N, Sharma RK. A novel approach for combating Klebsiella pneumoniae biofilm using histidine functionalized silver nanoparticles. Front Microbiol. 2017; 8: 1104.

13. Cheruvanachari P, Pattnaik S, Mishra M, Pragyandipta P, Naik PK. Terpinen-4-ol, an active constituent of kewda essential oil, mitigates biofilm forming ability of multidrug resistant *Staphylococcus aureus* and *Klebsiella pneumoniae*. J Biol Act Prod Nat. 2022; 12(5):406-420.
14. Luciardi MC, Blázquez MA, Cartagena E, Bardón A, Arena ME. Mandarin essential oils inhibit quorum sensing and virulence factors of *Pseudomonas aeruginosa*. LWT-Food Science and Technology, 2016; 68: 373-380.
15. Santoshi S, Naik PK (2014). Molecular insight of isotypes specific β-tubulin interaction of tubulin heterodimer with noscapinoids. J Comput-Aided Mol Des. 2014; 28: 751-763.
16. Caesar LK, Cech NB. (2019). Synergy and antagonism in natural product extracts: when 1+ 1 does not equal 2. Nat Prod Rep. 2019; 36(6): 869-888.

## Abbreviations

TTC: 2,3,5-triphenyltetrazolium chloride
TSB: Tryptic soya broth
DFT: Density functional theory
IPA: Ingenuity pathway analysis
FPKM: Fragments/kb of exon per million fragments mapped
DEGs: Database of essential genes
CRA: Congo Red Agar

**Supplementary Data**

**Supplementary Table 1. Phytochemical constituents identified in the crude methanolic leaf extract of *Cordia macleodii* through HRMS analysis.**

| Sl. | Name of the compound | Retention time | Molecular formula | m/z | Peak area (%) | Structure | Activities |
|---|---|---|---|---|---|---|---|
| 1. | Procyanidin B2 | 6.25 | $C_{30}H_{26}O_{12}$ | 579.1510 | 3.75 | 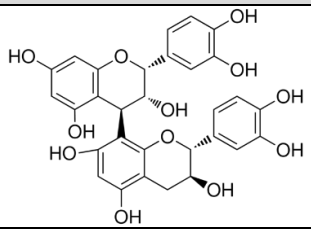 | Antibacterial |
| 2. | Brevione F | 8.17 | $C_{27}H_{32}O_5$ | 437.2302 | 1.52 | 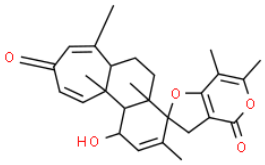 | Antiviral |
| 3 | Streptophenazine D | 8.32 | $C_{23}H_{26}N_2O_5$ | 411.1920 | 1.19 | 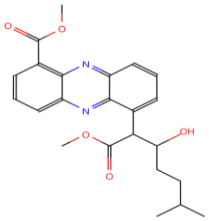 | Antibacterial |
| 4. | Ganosinensic acid A | 8.49 | $C_{27}H_{38}O_6$ | 459.2749 | 1.07 | 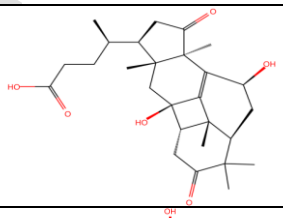 | Anti-tumor, Anti-inflammation, Antioxidant and Antimicrobial |
| 5. | Xeromphalinone F | 8.61 | $C_{29}H_{36}O_6$ | 481.2584 | 2.52 | 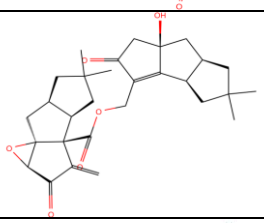 | Antibacterial, Antifungal |
| 6. | 1,2,3,4,5-Penta-O-acetyl-6-O-nonylhexitol | 8.87 | $C_{25}H_{42}O_{11}$ | 541.2619 | 1.50 | 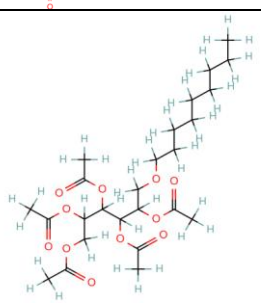 | -- |
| 7. | Ouabain | 9.24 | $C_{29}H_{44}O_{12}$ | 585.2902 | 0.63 | 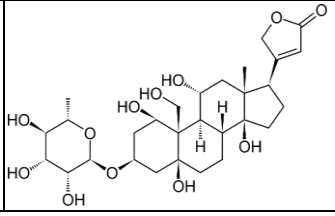 | Antibacterial |

| | | | | | | | |
|---|---|---|---|---|---|---|---|
| 8. | Xanthorin 8-O-β-D-gentiobioside | 9.57 | $C_{28}H_{32}O_{16}$ | 625.1794 | 0.80 | 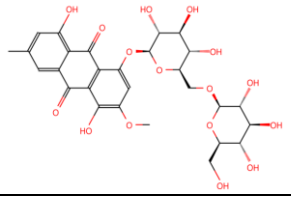 | Antibacterial |
| 9. | Methyl dichloroasterrate | 10.06 | $C_{18}H_{16}C_{l2}O_8$ | 453.0134 | 8.71 | 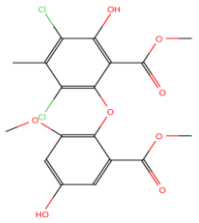 | Antifungal |
| 10. | Grifolinone B | 10.18 | $C_{44}H_{54}O_7$ | 717.3751 | 0.88 | 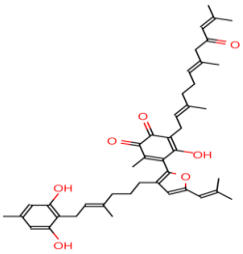 | Antimicrobial, anticancer |
| 11. | Penitalarin A | 10.56 | $C_{23}H_{34}O_4$ | 375.2528 | 0.15 | 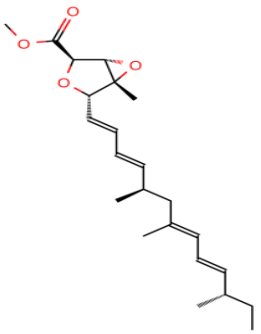 | Antimicrobial, Antifungal |
| 12. | 1α-chloro-2β-hydroxyeremophil-7(11),9-dien-8-one | 10.34 | $C_{15}H_{21}ClO_2$ | 291.1110 | 0.11 | 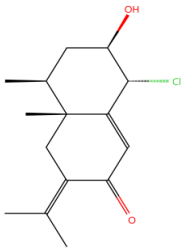 | -- |
| 13. | Pladienolide D | 10.94 | $C_{30}H_{48}O_9$ | 553.3384 | 0.16 | 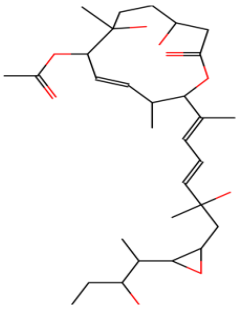 | Antibacterial, Anticancer |
| 14. | Collismycin B | 11.30 | $C_{13}H_{13}N_3O_2S$ | 298.0623 | 0.15 | 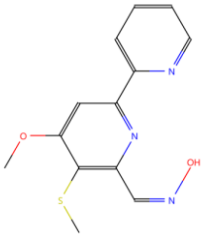 | Antibacterial, Antifungal |

| | | | | | | | |
|---|---|---|---|---|---|---|---|
| 15. | Tiliroside | 11.64 | $C_{30}H_{26}O_{13}$ | 595.1469 | 13.59 | 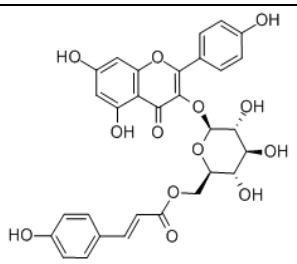 | Antibacterial, Antiprotozoal, Antidiarrheal, Antioxidant, Antiviral |
| 16. | Soraphen A1α | 11.94 | $C_{29}H_{44}O_8$ | 521.3102 | 6.18 | 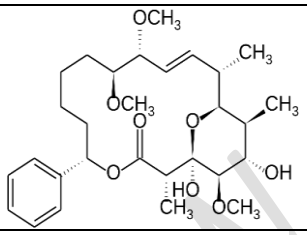 | Antifungal, Anticancer |
| 17. | Pseudoxylallemycin A | 12.68 | $C_{32}H_{44}N_4O_4$ | 549.3437 | 0.99 | 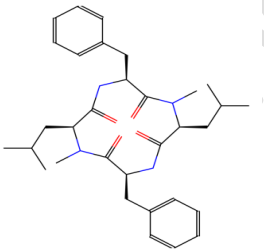 | Antibacterial |
| 18. | Arthripenoid B | 12.91 | $C_{30}H_{46}O_9$ | 551.3226 | 0.08 | 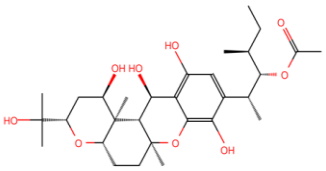 | -- |
| 19. | Stephensiolide A | 13.76 | $C_{28}H_{49}N_5O_9$ | 622.3425 | 0.18 | 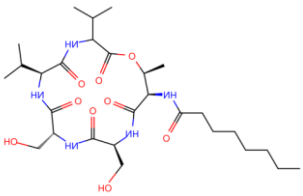 | Antibacterial |